Appl. Phys. 12, 45—53 (1977)

Applied Physics

Double Correlation Technique (DDLTS) for the Analysis of Deep Level Profiles in Semiconductors

H. Lefèvre and *M. Schulz*

Institut für Angewandte Festkörperphysik, Fraunhofer-Gesellschaft, D-7800 Freiburg, Fed. Rep. Germany

Received 18 August 1976/Accepted 6 September 1976

Abstract. A very sensitive technique is presented which can be applied to determine deep level profiles in space-charge layers of Schottky barriers or *pn*-junctions. The method uses an extended transient capacitance technique with correlation similar to Lang's DLTS technique. The extension of DLTS to double correlation DDLTS is necessary to resolve the deep level profile and to exclude the field dependence of the capture cross-section and contact effects. By using a double-pulse capacitance transient and correlation, these undesired effects can be subtracted. Profiles can be determined for deep levels at concentrations 10^4 times lower than the background doping. Results are reported for epitaxial GaAs which showed one major deep level at 0.18 eV below the conduction band. Near the interface to the substrate, a slight shift in energy from 0.18 to 0.19 eV is observed. A second level at 0.43 eV decays into the epi-layer in the form of a diffusion tail.

PACS Code: 06, 79.20, 73

Several papers on the measurement of deep level profiles have recently been published [1–6]. Most of these techniques are based on voltage dependent capacitance or admittance measurements. The evaluation normally is rather elaborate so that the measurements can only be employed on special test samples rather than for standard process control.

Lang's [1, 2] DLTS[1] method can easily be employed to analyse energy spectra and capture cross-sections in semiconductors by a correlation analysis of the deep level transient. This technique also proved very useful for the analysis of implanted deep levels [7].

In this paper, we have further developed this DLTS technique to obtain a higher sensitivity for the detection and analysis of deep levels. This sensitivity can then be traded with the spatial resolution of a profile measurement. The improved sensitivity is achieved by a *double* correlation in the DLTS technique. We therefore simply use the abreviation DDLTS for our method.

[1] DLTS = "Deep Level Transient Spectroscopy".

By this double correlation we can eliminate deleterious effects caused in the contact region and also exclude the smear out of the emission rate due to the field variation in the space charge region.

Measurement Technique

In the space charge layer of a Schottky barrier or a *pn*-junction, traps can be filled or emptied by varying the applied voltage. At a high reverse bias, a large number of traps are raised above the Fermi level. They emit their charge by thermal excitation. When a low reverse bias is applied most of the deep centers are located below the Fermi level. They are filled rapidly by capture of a charge carrier. The change of the charge state of the trap centers can be observed in the capacitance transient.

Traps in the upper half of the band gap respond to electrons in the conduction band and traps in the lower half respond to holes in the valence band. In a

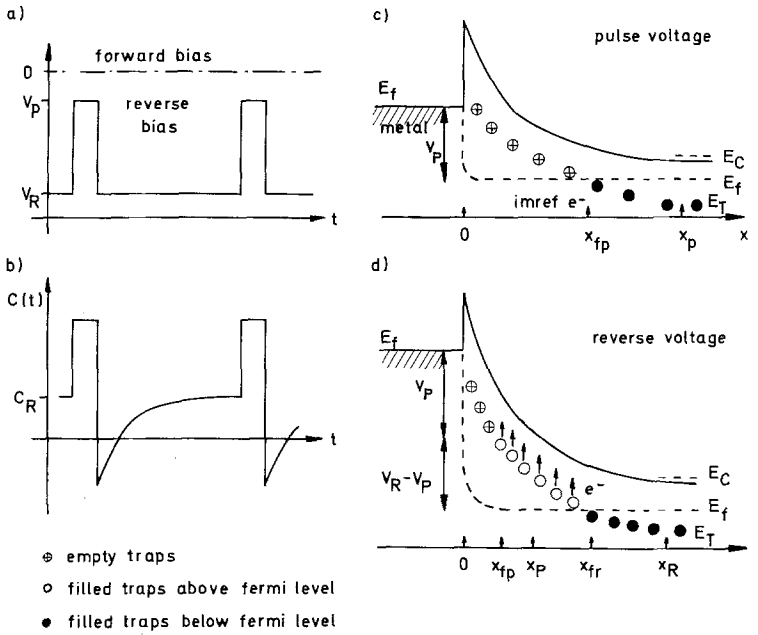

Fig. 1a—d. Schematic drawing of pulse sequence and energy band bending in a Schottky contact as used for the correlation analysis in DLTS. (a) time variation of the bias voltage; (b) time variation of the capacitance signal; (c) and (d) energy band bending at different bias situations

pn-junction, both types of traps can be investigated in the same device because both types of carriers are present simultaneously [1, 2]. In a Schottky barrier structure, only majority carriers are present. In order to investigate trap centers in the whole band gap *n*- and *p*-type material have to be investigated separately [3, 5, 8]. In our method we prefer to use Schottky barriers because they are easily fabricated on clean wafers without a hot processing stage. The evaluation is simpler than for a *pn*-junction because only one type of carrier is present.

The measurement procedure follows the DLTS technique [1, 2]. The basic pulse sequence, the observed capacitance signal and the energy band bending in the Schottky barrier [9] are shown in Fig. 1 for *n*-type material. Short compensating pulses are superimposed on the steady state reverse bias. During this pulse, the depth of the space charge layer is reduced. Traps which are not located within the reduced space charge layer are filled with a trapped charge. After the pulse, the filled traps emit their charge again with the thermal emission rate e_n [7, 10].

$$e_n = \frac{1}{\tau_e} = \sigma_n v_{\text{th}} N_c \exp[-(E_c - E_T)/kT], \tag{1}$$

where τ_e is the emission time constant, σ_n is the electron capture cross-section, v_{th} is the thermal drift velocity of electrons, N_c the effective density of states and $E_c - E_T$ the energy position of the trap center.

In DLTS, a spectrum of several deep levels can be resolved by correlating the transient capacitance signal with a known function [1, 7]. Peaks are observed in a temperature scan when the transient signal is of the magnitude of the characteristic time constant of the reference function. Normally the difference signal taken at two delay times t_1, t_2 is used to obtain a correlation. The maxima are then observed at the corresponding temperature for which $\tau_e = t_1/0.69$, when the signal is measured at t_1 and $t_2 = 2t_1$.

In this paper, we have improved this DLTS method by using double correlation called DDLTS. In DDLTS, two pulses of different height are used to charge trap levels in the space charge layer. In a first correlation, the transient capacitances after the two pulses are related to form the differences $\Delta C(t_1)$ and $\Delta C(t_2)$ at corresponding delay times after each pulse (see Fig. 2). In a second step the same correlation $\Delta C(t_1) - \Delta C(t_2)$ is performed as in DLTS to resolve a time constant spectrum in a temperature scan. This double correlation can easily be obtained with a four channel boxcar integrator or a multichannel correlator.

The special features of the double correlation are demonstrated in Fig. 3. The additional (first) correlation step sets an observation window $x'_{fp} - x_{fp}$ within the space charge layer. By forming the difference $\Delta C(t)$ of the capacitance transient after the pulses, only the charge recovery for traps in the observation window is detected. This procedure has several advantages:

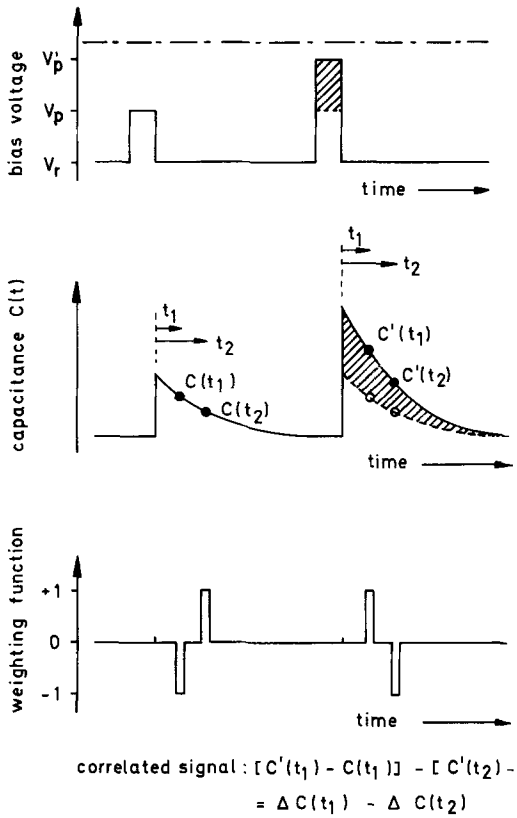

Fig. 2. Schematic drawing of the pulse shape, capacitance signal and correlation weighting function as used in DDLTS

1) All the traps in the observation window are located well above the majority carrier Fermi level. The transient obtained is entirely determined by the thermal emission rate. Traps located in the vicinity of the Fermi level which have a faster rate are excluded from the measurement.
2) All the traps in the observation window are exposed to approximately the same electrical field. In earlier measurements, indications for field dependent time constants are found [1, 7]. A smear-out of the time constant due to the field variation in the space charge layer is therefore avoided by the new technique. The exclusion of the field dependence is absolutely necessary when a profile analysis is performed by varying the applied bias voltage.
3) The double correlation leads to a further reduction of the measurement noise. By forming the difference, spurious signals caused in the contact region and by drift in the electronics are substracted.
The profile analysis is performed by varying the position of the observation window. The shift is obtained by varying the steady state reverse bias and keeping all the other parameters fixed. For small pulses, the field in and the width of the observation window vary only slowly by second-order effects which can be ignored in a first approximation. The profile of the deep levels can be determined by a straight forward computer evaluation.

Theory

The evaluation of the transient capacitance measurement is based on an integration of Poisson's equation to obtain the relation of the applied voltage V_r of the Schottky barrier to the various depths where the trap levels cross the Fermi level x_f and the boundary of the space charge region x_r

$$V_D+V_r=\frac{q}{\varepsilon}\int_0^{x_r(t)} x\{n_0(x)+(1-e^{-t/\tau})n_T(x)u[x_{fr}(t)-x]\}dx, \tag{2}$$

where

$$u(x)=\begin{cases}0 & \text{for } x\leqq 0\\ 1 & \text{for } x>0\end{cases} \tag{3}$$

is a step function, and q represents the elementary charge. V_D denotes the diffusion voltage, $n_T(x)$ is the trap concentration, x_{fr} is defined by the position where the trap level crosses the Fermi level (see Fig. 3). This position varies with time. At the end of the charging pulse when all the traps are filled, we obtain

$$V_D+V_p=\frac{q}{\varepsilon}\int_0^{x_p} x[n_0(x)+n_T(x)u(x_{fp}-x)]dx\,; \tag{4}$$

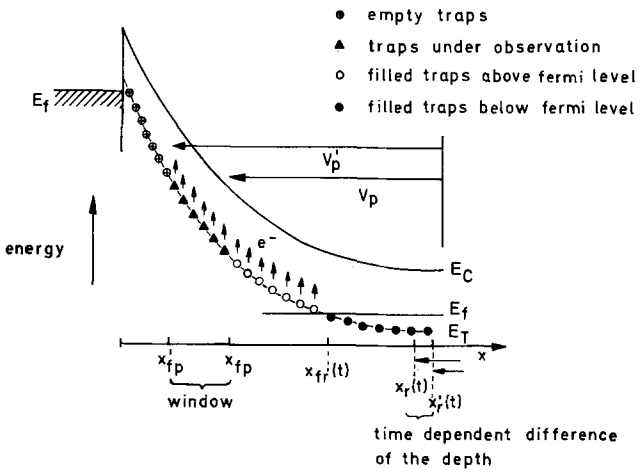

Fig. 3. Schematic drawing of the energy band bending in the Schottky contact for the definition of the Fermi level cross points and the observation window

V_p is the pulse voltage and x_{fp} is the position where the trap level crosses the Fermi level at the end of the pulse.
The charge transient is obtained by the implicit equation

$$V_r - V_p = \frac{q}{\varepsilon}\left[\int_{x_p}^{x_r(t)} x n_0(x)dx + \int_{x_{fp}}^{x_{fr}(t)} x n_T(x)(1-e^{-t/\tau})\right]dx. \tag{5}$$

Equation (5) can be used to obtain the relation for two different pulse heights V_p and V_p'

$$V_p' - V_p = \frac{q}{\varepsilon}\left[\int_{x_p}^{x_r(t)} x n_0(x)dx - \int_{x_p'}^{x_r'(t)} x n_0(x)dx\right] + \frac{q}{\varepsilon}(1-e^{-t/\tau}) \cdot \left[\int_{x_{fp}}^{x_{fp}'} x n_T(x)dx + \int_{x_{fr}'(t)}^{x_{fr}(t)} x n_T(x)dx\right], \tag{6}$$

where

$$\int_{x_{fp}}^{x_{fr}(t)} x n_T(x)dx = \int_{x_{fp}}^{x_{fp}'} x n_T(x)dx + \int_{x_{fp}'}^{x_{fr}'(t)} x n_T(x)dx + \int_{x_{fr}'(t)}^{x_{fr}(t)} x n_T(x)dx.$$

The second correlation forms the difference of the signal taken at two delay times t_1 and t_2. Using (6) this step results in

$$O = \underbrace{\int_{x_r(t_2)}^{x_r(t_1)} x n_0(x)dx - \int_{x_r'(t_2)}^{x_r'(t_1)} x n_0(x)dx}_{\mathrm{A}} + \underbrace{(e^{-t_2/\tau} - e^{-t_1/\tau}) \int_{x_{fp}}^{x_{fp}'} x n_T(x)dx}_{\mathrm{B}} + \mathrm{C} \tag{7}$$

$$\mathrm{C} = (1-e^{-t_1/\tau}) \int_{x_{fr}'(t_1)}^{x_{fr}(t_1)} x n_T(x)dx - (1-e^{-t_2/\tau}) \int_{x_{fr}'(t_2)}^{x_{fr}(t_2)} x n_T(x)dx.$$

Term A describes the change in depth of the space charge layer within the time difference which is necessary to compensate the change of the space charge due to thermal emission contained in term B. Term B is dependent on the pulse height V_p and V_p' chosen and the trap concentration contained in the observation window x_{fp}, x_{fp}'. Term C takes into account the feed back of the width of the space charge layer on the Fermi level cross points. This contribution can be neglected when the trap concentration and thus the change of the space charge layer width is small.
The integrals can be solved if average values are used within the boundaries

$$\begin{aligned}
\mathrm{A} &= \tfrac{1}{2}\bar{n}_0(x_r(t_2))[x_r'^2(t_2) - x_r^2(t_2)] \\
&\quad - \tfrac{1}{2}\bar{n}_0(x_r(t_1))[x_r'^2(t_1) - x_r^2(t_1)] \\
\mathrm{B} &= \tfrac{1}{2}(e^{-t_2/\tau} - e^{-t_1/\tau})\bar{n}_T(x_{fp})(x_{fp}'^2 - x_{fp}^2) \\
\mathrm{C} &= \tfrac{1}{2}(1-e^{-t_1/\tau})\bar{n}_T(x_{fr}(t_1))[x_{fr}^2(t_1) - x_{fr}'^2(t_1)] \\
&\quad - \tfrac{1}{2}(1-e^{-t_2/\tau})n_T(x_{fr}(t_2))[x_{fr}^2(t_2) - x_{fr}'^2(t_2)],
\end{aligned} \tag{8}$$

where the average values are taken in the regions:

$\bar{n}_0(x_r(t_i))$ constant in $[x_r(t_i), x_r'(t_i)]$ $\quad i=1,2$
$\bar{n}_T(x_{fp})$ constant in $[x_{fp}', x_{fp}]$
$\bar{n}_T(x_{fr}(t_i))$ constant in $[x_{fr}(t_i), x_{fr}'(t_i)]$ $\quad i=1,2$.

For the profile measurement it is convenient to use a large delay time t_2 so that $\exp(-t_2/\tau) \approx 0$. At this time the width of the space charge region is independent of the pulse height and $x_r(t_2) = x_r'(t_2)$ and $x_{fr}(t_2) = x_{fr}'(t_2)$.
Using (7) and (8) we obtain

$$\underbrace{\bar{n}_T(x_{fp})e^{-t_1/\tau}(x_{fp}'^2 - x_{fp}^2)}_{\mathrm{B}^*} + \mathrm{C}^* = \underbrace{\bar{n}_0(x_r(t_1))[x_r^2(t_1) - x_r'^2(t_1)]}_{\mathrm{A}^*} \tag{9}$$

and

$$\mathrm{C}^* = (e^{-t_1/\tau} - 1)\bar{n}_T(x_{fr}(t_1))[x_{fr}^2(t_1) - x_{fr}'^2(t_1)].$$

The contribution of the feed-back term C* vanishes for $t_1 = 0$. For $t_1 \neq 0$, it can normally be ignored when the deep doping concentration is small with respect to the shallow doping. The error then is given by

$$f_b = \frac{\mathrm{C}^*}{\mathrm{B}^*} = (1-e^{-t_1/\tau})\frac{x_{fr}^2(t_1) - x_{fr}'^2(t_1)}{x_{fp}'^2 - x_{fp}^2}\frac{\bar{n}_T(x_{fr}(t_1))}{\bar{n}_T(x_{fp})}. \tag{10}$$

Equation (9) can be solved for $n_T(x)$. By using $\Delta C(t_1) = C_r(t_1) - C_r'(t_1)$, $C_r = \frac{\varepsilon A}{x_r}$ and $\frac{1}{C_r^2(t_1)} - \frac{1}{C_r'^2(t_1)} \approx 2\frac{\Delta C(t_1)}{C_r^3(t_1)}$

$n_T(x)$ can be experimentally determined

$$\bar{n}_T(x_{fp}) = 2e^{t_1/\tau}(1+f_b)(\varepsilon A)^2 \cdot \left[\bar{n}_0(x_r(t_1))\frac{\Delta C(t_1)}{C_r^3(t_1)}\frac{1}{x_{fp}^2 - x_{fp}'^2}\right]. \tag{11}$$

The Fermi level cross-points x_{fr} can be derived from the band bending when the shallow doping profile is known

$$E_f - E_T = \frac{q^2}{\varepsilon} \int_{x_{fr}}^{x_r} (x_r - z) n_0(z) dz \,. \tag{12}$$

It is only assumed that the charging state of the trap level is determined by the majority carrier Fermi level. In half the band gap this can be assumed to be approximately true. All the other parameters of (11) are obtained by the DDLTS technique.

$C_r(t_1)$ and $C_r(t_1)$ are the capacitance values measured at time t_1 after the two pulses V_p and V_p', respectively. $\Delta C(t_1)$ is the double correlated capacitance signal.

The time constant of the trap level τ and the energy depth E_T are determined by the normal temperature scan procedure. The shallow doping profile is determined by using the CV-curve and by [12, 13]

$$n_0(x) = \frac{C_r^3}{q \varepsilon A^2} \frac{dV_r}{dC_r} \,. \tag{13}$$

Several deep levels can be separated by setting the measurement time constant t_1 and temperature T to the time constant τ of the level under investigation. All the trap levels which emit their charge faster than this time constant contribute only to static charge of the shallow doping. Levels which are deeper than the level under investigation are too slow to contribute to the correlation signal. In this manner, profiles can be determined for each level separately.

Experiment

Profile measurements were performed on n-type VPE GaAs epitaxial layers (thickness $\approx 5\,\mu m$) on a low resistivity substrate. The wafers were cut to test samples of approx. $0.5 \times 1.0\,cm^2$ size. The samples were etched back by an H_2O_2–NH_3–H_2O etch in order to be able to analyse trap levels in the bulk of the epilayer and near the substrate interface. The etch rate used was $1\,\mu m/45\,s$. The rate was measured mechanically by a Dectac.

Evaporated gold dots (0.5 mm ∅) were used as Schottky barrier structures. The substrate surface was completely evaporated with gold. The shallow doping profile was determined by using a standard laboratory profiler [11].

A block diagram of the DDLTS setup is shown in Fig. 4. This setup contains the same basic circuit as used in DLTS [1, 2, 7]. The sample is mounted in a bridge circuit with phase shifter and attenuator to balance the steady state 30 MHz signal of $\lesssim 10\,mV$ amplitude. The steady state reverse bias is connected to one port of the sample, the pulsed signal to the other one.

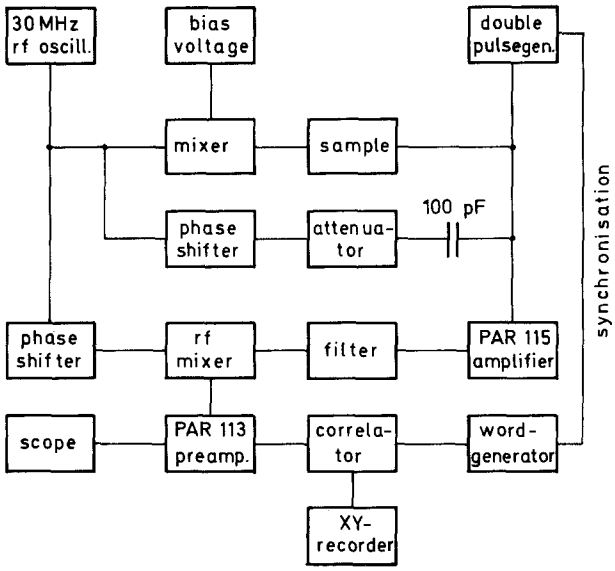

Fig. 4. Block diagram of the measurement setup of DDLTS

The offset signal of the bridge observed after the pulses, is amplified, phase-sensitively detected and fed into a correlator or four-channel boxcar averager. The phase-sensitive detection was adjusted so that the capacitive mode was only measured. The desired correlation was formed by multiplication with the weighting function, as shown in Fig. 2. The sensitivity was calibrated by comparing a known capacitance signal with a commercial bridge. The sensitivity was so high that a capacitance change of the order of 0.001 pF could still be detected out of the noise. The measurement temperature could be varied between 45 and 310 K by a closed-cycle Air Products refrigerator.

Results

The profile of compensated shallow donors of the GaAs wafer under investigation is shown in Fig. 5. The profile is composed by six measurements taken after different back etching steps. The sections match fairly well although the measurements were taken in different parts of the wafer.

The doping of the epilayer is quite uniform. However, slight ripples with an amplitude of about 5% of the doping concentration are observed. The period of these

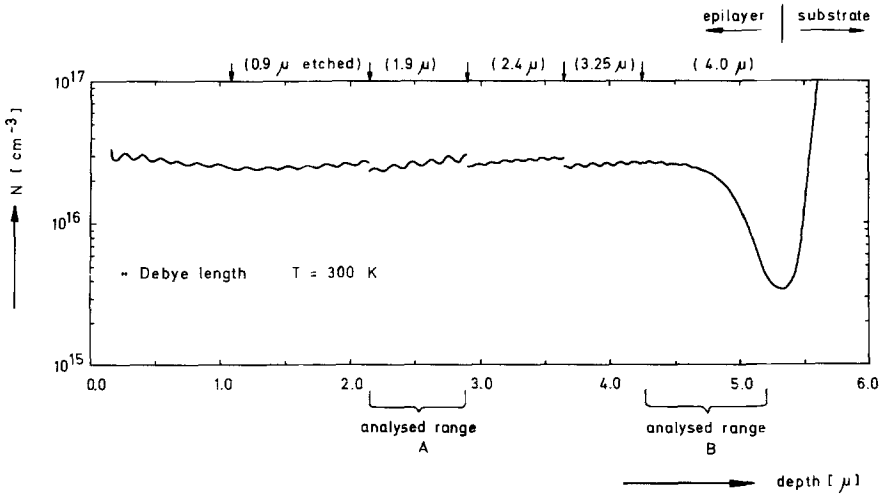

Fig. 5. Free carrier concentration profile through the epitaxial layer. The profile was composed by 6 different measurements taken after various etching steps. The ranges where deep level profiles are taken are marked by the brackets A and B

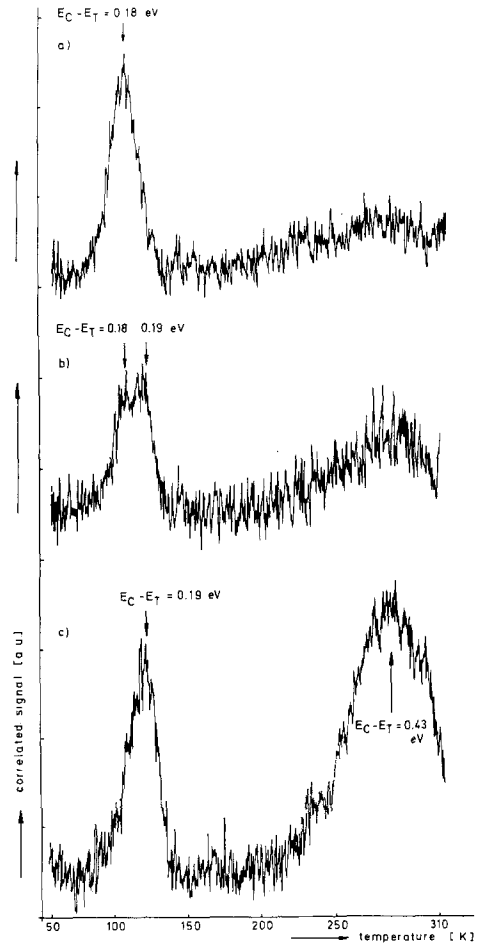

Fig. 6a—c. Temperature scans of the DDLTS correlation signals (a) observation window set at 2.5 μm depth in range A; (b) observation window set at 4.5 μm depth in range B; (c) observation window set at 5.0 μm depth in range B. Energy values determined for the observed peaks are marked in the plot

ripples corresponds to the growth rate of the layer and the period of the rotation during growth. They are obviously caused by a slight temperature inhomogeneity across the wafer in the reactor. Near the interface with the substrate, the well-known trough is observed in the doping concentration. No buffer layer was grown in this wafer. Trap level spectra were measured at the marked positions in the bulk of the epilayer and in the vicinity of the interface.

Temperature scans of the double correlation signal are shown in Fig. 6a–c. Spectrum a) was taken with the observation window positioned at a depth of about 2.5 μm. A strong peak is observed at 110 K. At high temperatures no distinct peak but rather a broad shoulder is observed. At a depth of 4.5 μm (1 μm from the interface) the peak at 110 K shows a distinct splitting with peaks at 110 and 120 K. The shoulder at high temperatures is increased. In the interface region two dominant peaks at 120 and 290 K are visible. The splitting disappeared.

By using the double correlation technique, the two peaks at low temperatures in Fig. 6b could be clearly separated. The peaks also show the typical asymmetry with a tail at low temperatures. The shape and width are in accordance with the theoretical relation

$$f(T)=(e^{-t_1/\tau}-e^{-t_2/\tau}) \quad \text{with} \quad \tau\sim e^{+\Delta E/kT}.$$

Using the single correlation (DLTS), the peaks were broader than expected from the theory.

The emission rates for each peak in the temperature scan are shown in Fig. 7 in an Arrhenius plot in order to obtain the activation energies and capture cross-

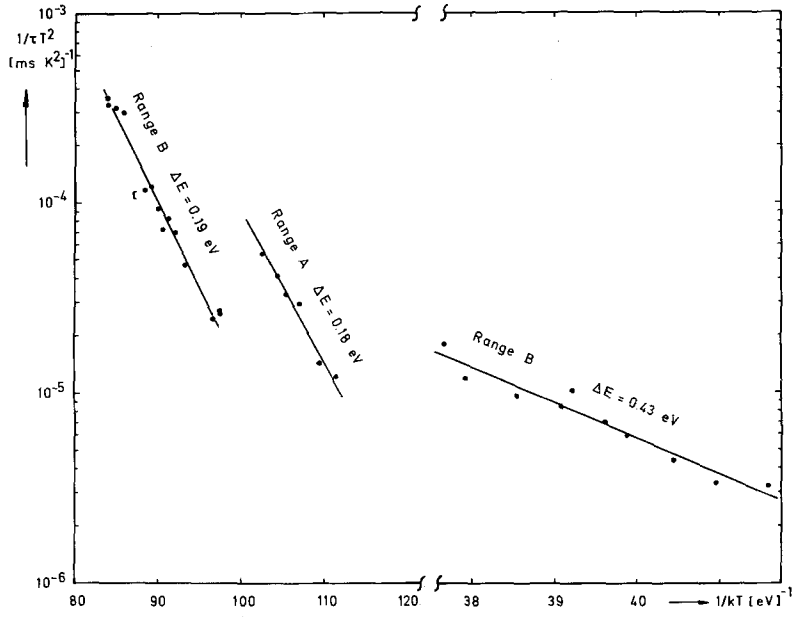

Fig. 7. Arrhenius plots of the emission time constants for the determination of the activation energy. The temperature dependence of the effective density of states in the conduction band and the thermal velocity of electrons are taken into account

sections. The values determined are shown in the figure. The capture cross-section was independent of temperature within the temperature range where the measurement is possible (± 20 K). The obtained data can be used to determine the deep level profile by using (11).

Figure 8 shows a typical result of the correlation signal $\Delta C(t_1)$ as a function of the pulse height. For small pulses the signal disappears in the noise. In the range 2–5 volts the signal is proportional to the pulse height.

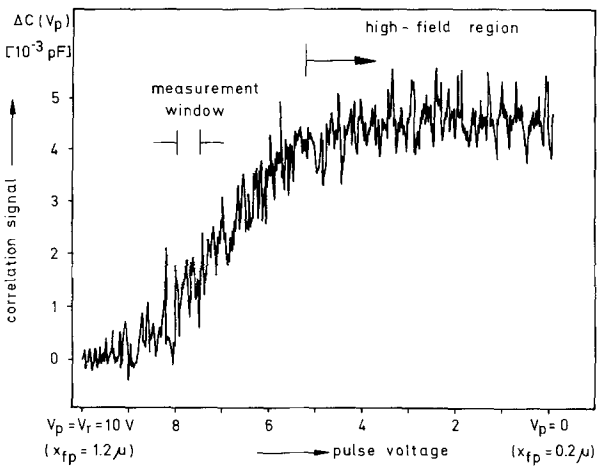

Fig. 8. Correlation signal as a function of the pulse height. The pulse heights for the optimal setting of the observation are marked in the insert

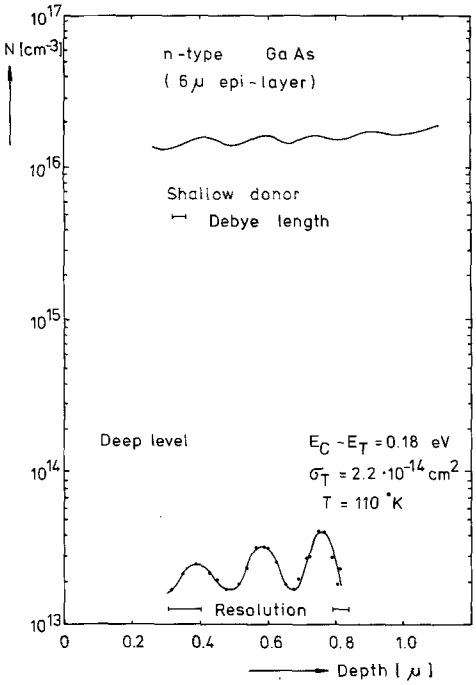

Fig. 9. Deep level profile as determined in range A of the GaAs sample. The depth scale is given with reference to the etched surface

For high pulses the emission time constant is field dependent and does not contribute to the signal. The correlation signal saturates. The observation window is therefore optimal if the pulse height is set to 2–3 volts.

Deep level profiles are obtained by varying the steady state reverse bias and keeping the pulse voltage fixed. Results for the GaAs wafer are shown in Figs. 9 and 10. The profile in Fig. 9 was taken in the bulk of the epitaxial layer for the level at 0.18 eV. The shallow donor profile is also shown for comparison. The deep level profiles shows the same fluctuation as the shallow doping, but at a higher amplitude. The maxima are in phase.

The resolution of the profile determination is also marked. It is calculated from the position of the Fermi level cross points. It is slightly dependent on the position in the profile. Since the resolution is of the order of the fluctuation period, the amplitude probably is even higher than determined in the analysis. The effect of the resolution can be seen in the drop of the wave amplitude towards the surface where the resolution is also decreased.

Profiles in the vicinity of the interface are shown in Fig. 10 for two deep levels at 0.19 and 0.43 eV together with the shallow doping profile. The profiles cannot be obtained right to interface because the Fermi level cross points do not reach the highly doped regions. The separation distance is larger for the deeper level.

The behaviour of the two deep levels is completely different. The concentration of the deep level decays into the epilayer while the profile of the shallow level is almost constant into the interface region. However, the fluctuation is still present although it disappears in the free carrier profile. The free carrier profile obviously is strongly compensated so that the fluctuations are covered by the interface effect. It is not quite clear whether the deep level shows a maximum or continuously decays into the epilayer. The measurement close to the interface is critically dependent on the free carrier profile in the interface which rises steeply into the substrate.

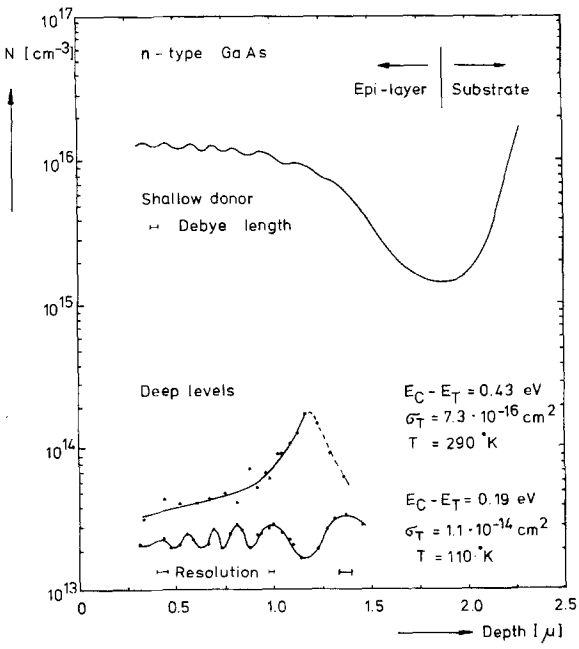

Fig. 10. Deep level profile as determined in range B of the GaAs sample. The depth scale is given with reference to the etched surface

Conclusions

We have presented a new technique DDLTS to analyse the properties of deep levels in semiconductors by double correlation of the transient capacitance. The technique can be applied to Schottky barriers and *pn*-junctions. It is an extension of Lang's DLTS technique.

The energy levels, capture cross-sections and the doping profiles can be determined in a standard procedure which is suitable as a routine laboratory setup. The properties can be obtained separately for each level if more than one deep level is present.

The results shown for GaAs demonstrate the resolution and sensitivity of DDLTS. Profiles can be determined for deep levels which have a concentration 10^4 times lower than the free carrier concentration. In high resistivity material, concentrations as low as 10^{10} cm^{-3} can be detected. The spatial resolution in the profile measurement is dependent on the concentration ratio and the sensitivity. It is of the order of 5% of the maximum space charge layer width.

The advantages of DDLTS are achieved by the double correlation which sets an observation window in the space charge layer. This observation window excludes surface effects and the field dependence of the emission rate. The observation window can be positioned into a region where the signal shows a maximum. The signal to noise ratio and thus the sensitivity of the technique are therefore also improved.

The results for GaAs are shown as examples for the technique. The fluctuations in the doping concentration demonstrate the feasibilities of the method. In the meantime results have been obtained for $GaAs_{0.6}P_{0.4}$ and transmutation-doped silicon which will be published separately. The deep level (0.43 eV) observed in GaAs near the interface probably is caused by interdiffusion of an impurity from the substrate into the epilayer during the growth of the layer. The tail corresponds to a diffusion constant of the order of

10^{-12} cm^2/s. This level could be partially responsible for the trough in the free carrier concentration. The low capture cross-section (7.3×10^{-16} cm^2) indicates the repulsive potential of an acceptor state. The level at 0.18 eV obviously is related to the temperature fluctuation and rotation during growth of the epilayer. Since the free carrier concentration has a maximum where also is a maximum in the trap profile the deep level obviously is of donor type. The higher capture cross-section (2.2×10^{-14} cm^2) than for the deep level is in accordance with this behaviour and the field dependence of the capture cross-section which can be explained as Frenkel-Poole effect on the emission of electrons [8, 14]. In the vicinity of the interface, this trap shows a slightly higher energy (0.19 eV) and a lower capture cross-section (1.1×10^{-14} cm^2). This effect is not completely understood. It might be related to strain in the interface.

Acknowledgement. The work was supported by a Ministry of Science and Technology contract. The authors alone are responsible for the scientific content.

References

1. D.V. Lang: J. Appl. Phys. **45**, 3014, 3023 (1974)
2. D.V. Lang, L.C. Kimerling: Proc. Intern. Conf. Lattice Defects in Semiconductors (1974), Institute of Physics Conf. Ser. No. 23, London, pp. 581
3. T. Ikoma, B. Jeppson: Proc. Intern. Symp. Gallium Arsenide and Related Compounds (1972), Institute of Physics Conf. Ser. No. 17, London, pp. 75
4. Gary H. Glover: IEEE Trans. ED-**19**, 138 (1972)
5. M. Schulz: Appl. Phys. Lett. **23**, 31 (1973)
6. M. Beguwala, C.R. Crowell: Sol. St. Electron. **17**, 203 (1974)
7. K. Nagasawa, M. Schulz: Appl. Phys. **8**, 35 (1975)
8. A.G. Milnes: *Deep Impurities in Semiconductors* (Wiley-Interscience, New York 1973)
9. M. Schulz: Proc. Europ. Summer School Scientific Principles of Semiconductor Technology (1974), European Physical Society, Bad Boll, pp. 191
10. W. Schockley, W.T. Read: Phys. Rev. **87**, 835 (1952)
11. G.L. Miller: IEEE Trans. ED-**19**, 1103 (1972)
12. C.O. Thomas, D. Kalny, R.C. Manz: J. Electrochem. Soc. **109**, 1055 (1962)
13. J. Hilibrand, R.D. Gold: R.C.A. Rev. **21**, 245 (1960)
14. J.R. Yeargan, H.L. Taylor: J. Appl. Phys. **39**, 5600 (1968)